RESEARCH ARTICLE

As low as diagnostically acceptable dose imaging in maxillofacial trauma: a reference quality approach

[1]Gerlig Widmann, [1]Hannes Schönthaler, [2]Alexander Tartarotti, [1]Gerald Degenhart, [3]Romed Hörmann, [1]Gudrun Feuchtner, [2,4]Reinhilde Jacobs and [2,5,6]Ruben Pauwels

[1]*Department of Radiology, Medical University of Innsbruck, Innsbruck, Austria;* [2]*Department of Imaging and Pathology, OMFS-IMPATH Research Group, KU Leuven and Oral and Maxillofacial Surgery, University Hospitals Leuven, Leuven, Belgium;* [3]*Division of Clinical and Functional Anatomy, Medical University of Innsbruck, Innsbruck, Austria;* [4]*Department of Dental Medicine, Karolinska Institutet, Stockholm, Sweden;* [5]*Aarhus Institute of Advanced Studies, Aarhus University, Aarhus, Denmark;* [6]*Department of Radiology, Faculty of Dentistry, Chulalongkorn University, Bangkok, Thailand*

Objectives: As-low-as-diagnostically-acceptable (ALADA) doses are substantially lower than current diagnostic reference levels. To improve dose management, a reference quality approach was tested in which phantom quality metrics of a clinical ALADA dose reference protocol were used to benchmark potential ALADA dose protocols for various scanner models.

Methods: Spatial resolution, contrast resolution, contrast-to-noise ratio (CNR) and subjective noise and sharpness were evaluated for a clinical ALADA dose reference protocol at 80 kV and 40 mA (CTDIvol 2.66 mGy) and compared with test protocols of two CT scanners at 100 kV and 35 mA (3.08–3.44 mGy), 80 kV and 54–61 mA (2.65 mGy), 80 kV and 40 mA (1.73–1.92 mGy), and 80 kV and 21–23 mA (1.00–1.03 mGy) using different kernels, filtered backprojection and iterative reconstructions. The test protocols with the lowest dose showing quality metrics non-inferior to the reference protocol were verified in a cadaver study by determining the diagnostic accuracy of detection of maxillofacial fractures and CNR of the optical nerve and rectus inferior muscle.

Results: 36 different image series were analysed in the phantom study. Based on the phantom quality metrics, potential ALADA dose protocols at 1.73–1.92 mGy were selected. Compared with the reference images, the selected protocols showed non-inferiority in the detection and classification of maxillofacial fractures and non-inferior CNR of orbital soft tissues in the cadaver study.

Conclusions: Reference quality metrics from clinical ALADA dose protocols may be used to guide selection of potential ALADA dose protocols of different CT scanners.
Dentomaxillofacial Radiology (2023) **52**, 20220387. doi: 10.1259/dmfr.20220387

Introduction

Dose optimisation in computed tomography (CT) continuously searches for "as low as reasonably achievable (ALARA)" or "as low as diagnostically acceptable" (ALADA) doses. Unfortunately, the optimum dose for each manufacturer, scanner, protocol, and reconstruction technology remains unknown for various diagnostic tasks. Diagnostic reference levels (DRLs) may act as trigger levels to initiate dose reductions.[1] However, they do not specifically address differences between scanners or lag behind the latest inventions in dose saving technology, including iterative reconstruction and deep-learning reconstruction.[2] As an example, in maxillofacial

CT diagnostic images, it has been shown that doses of only 5% of current DRLs can be acceptable.[3–5] Equally important to focusing on dose is comparing image quality between scanners and protocols. Image quality metrics such as spatial resolution, contrast resolution and noise may be evaluated using image quality phantoms.[6,7] Recently, a clinical ALADA dose protocol for maxillofacial trauma using a volume computed tomography dose index of (CTDIvol) of 2.66 mGy has been introduced in clinical routine.[8,9] It is theorized that once the phantom quality metrics of the clinical ALADA dose protocol are known, the corresponding ALADA dose protocols for other devices may be obtained by comparative phantom testing. Therefore, the objective of this study was a) to define the phantom image quality metrics of this clinical ALADA dose reference protocol, b) to compare the reference image quality metrics to those obtained from various protocols of two different test scanners, and c) to verify potential ALADA dose protocols from the two test scanners, which demonstrated phantom quality metrics that were non-inferior to the reference protocol, by determining the diagnostic accuracy of detection of maxillofacial fractures and contrast-to-noise-ratios of the optical nerve and rectus inferior muscle in a cadaver study.

Methods

Test phantom
The image quality phantom (SEDENTEXCT IQ phantom, Leeds Test Objects Ltd, Boroughbridge, UK) is a cylindrical customised polymethyl methacrylate (PMMA) phantom, which represents an adult head (diameter 16.0 cm, height 17.7 cm).[6,7,10] The phantom contains one central and six peripheral holes for the placement of various inserts (3.5 cm diameter, 2 cm height). The following inserts were selected:

(1) Line-pair inserts: alternating aluminium and polymer sheets with different thicknesses, ranging from one line pairs per millimetre (lp mm-1) to 10 lp mm-1 for an evaluation in the axial (xy) and transaxial (xz/yz) planes.
(2) Contrast resolution inserts: two different densities of hydroxyapatite (HA): 100 mg cm^{-3} and 200 mg cm^{-3}. For each density, five cylindrical rods of different diameters (1–5 mm) are positioned at the vertices of a regular pentagon, using PMMA as a background material.
(3) Contrast-to-noise ratio inserts: five cylindrical rods 1.0 cm in diameter and containing air, aluminium or two different densities of hydroxyapatite (HA): 100 mg cm^{-3} and 200 mg cm^{-3}, using PMMA as background material.

CT imaging
The test phantom was scanned using the CT scanners and protocols given in Table 1. The ALADA dose reference protocol at CTDI$_{vol}$ 2.66 mGy using FBP with bone and standard kernel of the reference scanner (64-row Discovery CT750 HD, GE Healthcare, Chicago, Illinois, United States of America) was compared with various protocols from test scanner 1 (64-row Somatom Definition AS, Siemens Healthineers, Erlangen, Germany) and test scanner 2 (128-row Somatom Definition Flash,

Table 1 Scanners and scan protocols.

Scanner	Collimation (mm)	kV	mA	CTDIvol (mGy)	Pitch	Rotation time (s)	Slice thickness (mm)	Convolution kernel	Reconstruction technology
Reference scanner	20 × 0.625	80	40	2.66	0.5	0.5	0.6	bone, standard	FBP
								standard, NR40	VEO
Test scanner 1	19.2 × 0.6	100	35	3.44	0.5	0.5	0.6	H60f, H30f	FBP
		80	54	2.65	0.5	0.5	0.6	H60f, H30f	FBP
		80	40	1.92	0.5	0.5	0.6	H60f, H30f	FBP
		80	21	1.03	0.5	0.5	0.6	H60f, H30f	FBP
Test scanner 2	38.4 × 0.6	100	35	3.08	0.5	0.5	0.6	H60f, H30f	FBP
								J45f, J30f	SAFIRE 3, SAFIRE 5
		80	61	2.65	0.5	0.5	0.6	H60f, H30f	FBP
								J45f, J30f	SAFIRE 3, SAFIRE 5
		80	40	1.73	0.5	0.5	0.6	H60f, H30f	FBP
								J45f, J30f	SAFIRE 3, SAFIRE 5
		80	23	1.00	0.5	0.5	0.6	H60f, H30f	FBP
								J45f, J30f	SAFIRE 3, SAFIRE 5

FBP, Filtered back projection; SAFIRE, Sinogram-affirmed iterative reconstruction; VEO, model-based iterative reconstruction.

Siemens Healthineers, Erlangen, Germany). In addition to filtered back projection (FBP), model-based iterative reconstruction VEO (GE Healthcare) and sinogram-affirmed iterative reconstructions SAFIRE three and SAFIRE 5 (Somatom Definition Flash) were used. All images were exported in digital imaging and communications in medicine format (DICOM) into IMPAX EE (Agfa HealthCare, Antwerp/Mortsel, Belgium) picture archiving and communication system (PACS) for image analysis.

No information regarding the scanner, dose and or reconstruction technique was available in the images. The images were read on high-resolution (three megapixel, DIN 6868–157 conformity), diagnostic colour-LCD monitors (RadiFOrce RX350, EIZO Europe GmbH, Mönchengladbach, Germany) in dimmed light conditions using a pre-set window/level of 500/4000 for the evaluation of the spatial resolution and 300/2500 for the evaluation of the contrast resolution. The readers were allowed to adjust the window/levels and to change magnification levels.

Phantom image quality metrics
Spatial resolution, contrast resolution and contrast-to-noise ratio were evaluated by a sixth-year medical student using the method described previously, for which excellent intraobserver and good to excellent interobserver agreement were published.[6,7] Subjective noise and sharpness were read in consensus by two readers, a sixth-year medical student and an expert head and neck radiologist with more than 10 years of experience.

Spatial resolution
The total number of clearly separable lines of the insert was counted in the sharp kernel images.

Contrast resolution
The number of visible rods for each insert containing the three different densities of HA was counted, with possible scores ranging between 0 (no rods visible) and 5 (all rods visible).

Contrast-to-noise ratio (CNR)
A circular region of interest (ROI) of 47 mm^2 was placed within all six materials inside the inserts and the PMMA insert as background to evaluate Mean Hounsfield Units (MHU) and standard deviation (SD). The CNR of each material *m* was calculated using the following formula.[7]

$$CNRm = \frac{|MHUm - MHUPMMA|}{\sqrt{SD_m^2 + SD_{PMAA}^2}}$$

Subjective noise and sharpness
Blinded test images of representative slices of the phantom inserts were displayed side-by-side with the reference image. Sharp and soft kernel images were compared to the reference bone and standard kernels, respectively. A 5-step grading scale was used: −2: much worse than reference; −1: slightly worse than reference; 0: equal to reference; +1: slightly better than reference; and +2: much better than reference.

Suggested ALADA dose protocols of the test scanners
The image quality metrics of the test protocols were descriptively compared to the image quality metrics of the reference images. For each of the test scanners, the protocol with the lowest dose providing non-inferior phantom image quality metrics was suggested as ALADA dose protocol.

Cadaver verification of the suggested ALADA dose protocols
The study was approved by the legal and ethical framework of the Medical University of XXX for studies on human cadavers.[11,12] The bodies were donated by people who had given their informed consent for their use for scientific and educational purposes prior to death. Two cadaver heads with intact soft tissues were used. The cadavers have been preserved using an arterial injection of an alcohol–glycerine solution and immersion in phenolic acid in water for 1–3 months.[13] To obtain maxillofacial fractures from simulated trauma the cadaver heads were injured to the midface, the temporal bone, the frontal bone, the parietal bone and the occipital bone using a hammer (impacts see Table 3).

The cadaver heads were scanned using the clinical ALADA reference protocol and the test protocols of scanner 1 and 2 using 2.65 mGy and the suggested ALADA dose protocols at 1.73 and 1.92 mGy, respectively (Table 1 and Table 4).

Fracture classification
Fractures were classified using the AO comprehensive injury automatic classifier (AO COIAC), a free computer software developed by the AO foundation.[14] This classification codes the first level on the coarse location of the fracture, the second level on the exact location of the fractures in the predefined regions, and the third level on special sub regions and relevant morphological characteristics like fragmented or none fragmented. Fracture classification was independently performed by two readers (medical students in their sixth year) following training of CT reading and fracture classification. The results for each image series were compared to the fracture classification from the reference images by an expert head and neck radiologist with more than 10 years of experience.

Contrast-to-noise ratio (CNR) of orbital soft tissues
CNR of the optical nerve (ON) and inferior rectus muscle (IRM) of one side-of each cadaver was evaluated on synchronized identical slice positions of the soft kernel images using a circular ROI placed on three consecutive slices using fat as the background tissue, as described in a previous publication.[9]
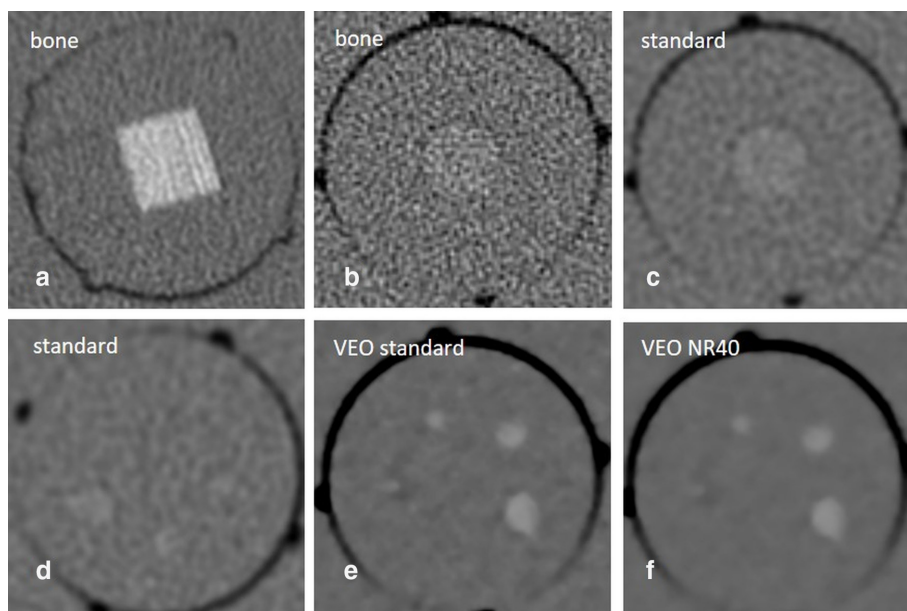
Figure 1   Phantom images from the reference scanner using the ALADA dose reference protocol at 2.66 mGy. A - Line-pair insert, showing four lp mm-1. B and C - Contrast-to-noise ratio insert hydroxyapatite (HA) 100 mg cm-3. D-F - Contrast resolution insert HA 100 mg cm-3, showing scores of 3/5 for FBP standard kernel, and 4/5 for both VEO standard and VEO NR40.

Data analysis
For data analysis and statistics, IBM SPSS Statistics 24 (IBM Corporation, Armonk, NY, USA) was used. ANOVA with repeated measures was used ($\alpha = 0.05$) for comparison of the CNR of the ON and IRM between the FBP standard kernel reference images and the test protocols.

Results

Phantom quality metrics
36 different image series from three different CT scanners were descriptively analysed in the phantom study.

Spatial resolution: The sharp kernel reference images allowed detection of 4 lp mm-1. The test scanner images allowed detection of only two lp mm-1 using doses of 3.08–3.44, 2.65, and 1.73–1.92 mGy. Test scanner images at 1.00–1.03 mGy could not discriminate line-pairs (compare Figures 1 and 2). SAFIRE did not improve visibility of individual lines.
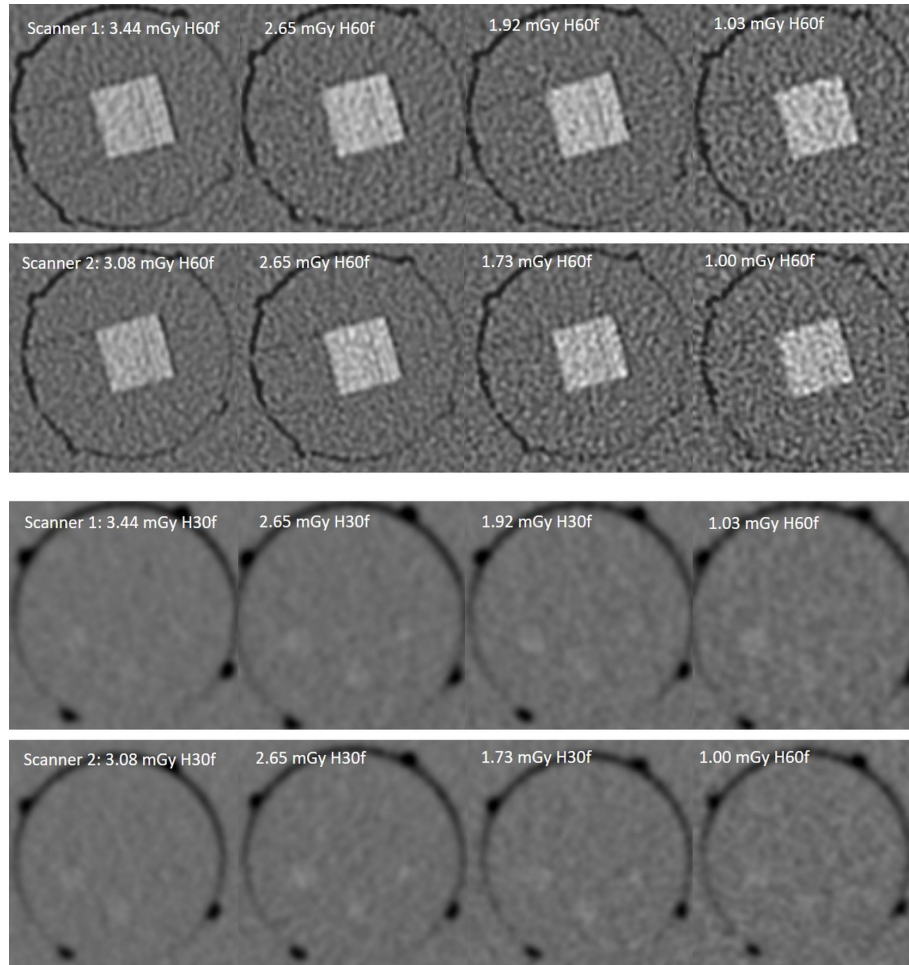
Contrast resolution: The soft kernel reference images showed scores of 3/5 HA-100, and 4/5 HA-200. Similar results were obtained by the FBP test scanner images using doses of 3.08–3.44, 2.65, and 1.73–1.92 mGy. At doses of 1.0–1.03 mGy, only a score of 2/5 HA-100, and 3/5 HA-200 was achieved. SAFIRE could not improve contrast resolution scores. VEO outperformed FBP and achieved the maximum scores in each group showing 4/5 HA-100, and 5/5 HA-200 (Figure 1).

Contrast-to-noise ratio (CNR):   CNR differed substantially between sharp and soft kernels and between FBP and iterative reconstructions (Table 2). Compared to the soft kernel reference images the HA-100 and HA-200 inserts showed comparable or higher CNR only by the FBP soft kernel images of the test scanners using doses of 3.08–3.44, 2.65, and 1.73–1.92 mGy. In the sharp kernel images, comparable or higher results were only achieved using SAFIRE. SAFIRE three improved CNR of the HA inserts over the FBP images by approximately 1.4 times and SAFIRE 5 by 1.8 times. SAFIRE 3 and 5 reduced noise by approximately 30 and 48%, respectively. VEO improved overall CNR of the HA inserts over FBP by approximately 3.9 times using standard and 6.4 times using NR40 kernel. VEO standard kernel and VEO NR40 kernel showed a noise reduction of about 71% and 84%.

Subjective noise and sharpness: Compared to the reference images, lower sharpness scores (−1) were found in all the FBP and SAFIRE images of the test protocols, with equal results obtained with FBP, SAFIRE three and SAFIRE 5. SAFIRE 3 and 5 scored slightly better than reference (+1) for noise. VEO standard kernel and VEO NR40 kernel, scored much better than reference (+2) for both noise and sharpness.

Suggested ALADA dose protocols of the test scanners: The following reference quality metrics were defined: spatial resolution two lp mm-1 (because in the test scanners only 2 lp mm-1 were detected even using higher doses); contrast resolution score 3/5 HA-100 and 4/5 HA-200; CNR 1.74 HA-100 and 4.40 HA-200. The suggested ALADA dose protocols of the test scanners were the protocol at 1.92 mGy for scanner 1, and 1.73 mGy for scanner 2.

Figure 2 Test scanner images of the line-pair and contrast resolution insert HA 100 mg cm-3.

Cadaver verification of suggested ALADA dose protocols

Fracture classification: Compared to the reference images, no clinically relevant difference regarding the AO-classification code was found for the suggested ALADA dose protocols at 1.73 and 1.92 mGy (Figure 3). Compared to the classification by the expert radiologist based on the reference images, the two non-expert readers provided only minor and non-clinically relevant differences of the classification or subclassification code (level 3) (Table 3). The reasons were differences in selecting the exact anatomical level 3 location of the classification system, interpreting the length of the fracture. For the frontal left impact of the cadaver head 1, observer one determined an additional classification code, because of a bony canal that was mistaken as a fracture.

Contrast-to-noise ratio (CNR) of orbital soft tissues: The standard kernel reference images showed a mean (SD-standard deviation) CNR of 2.8 (SD 1.72) for the optical nerve (ON) and 2.36 (SD 1.14) for the inferior rectus muscle (IRM) (Table 4). Compared to the reference images, similar or higher results were obtained

in the ALADA dose protocols of both test scanners and there was no statistically significant difference. SAFIRE increased CNR of the ON by 44.2% and IRM by 73.4%. VEO had statistically significant higher CNR than FBP and showed an increase in CNR of the ON even by 247.6% and of the IRM by 184.9%. (Table 3 and Figure 4).

Discussion

In CT of maxillofacial trauma, simple adherence to protocols keeping doses within national DRL (para-nasal sinuses 8–12 mGy[15,16] must not be mistaken with following the ALARA/ALADA principle. Furthermore, a simple focus on dose does not reflect differences in scanners and reconstructive algorithms, which means that the ALADA dose protocol of older scanners may significantly differ from the ALADA dose protocol of latest generation scanners, and may differ between vendors.[17] Sufficient image quality is of utmost importance for setting up ALADA dose protocols. Requirements on diagnostic image quality in maxillofacial CT

**Table 2** Contrast-to-noise ratios for five test materials in images obtained with the test protocols.

Scanner	CTDIvol (mGy)	Reconstruction technology	Sharp kernels l Soft kernels			
			AIR	ALU	HA-100	HA-200
Reference scanner	2.66	FBP	4.33/12.42	10.82/16.70	0.48/1.74	1.21/4.40
		VEO standard	n.a. / 38.31	n.a. / 77.58	n.a. / 6.72	n.a. / 19.23
		VEO NR40	n.a. / 49.93	n.a. / 96.04	n.a. / 11.07	n.a. / 30.70
Test scanner 1	3.44	FBP	5.49/28.41	7.34/23.07	0.39/2.38	1.17/6.00
	2.65	FBP	4.27/26.18	8.37/14.04	0.42/2.43	0.99/6.47
	1.92	FBP	3.75/15.46	7.63/12.74	0.35/2.08	0.88/4.41
	1.03	FBP	2.57/13.14	5.78/11.55	0.31/1.51	0.75/4.07
Test scanner 2	3.08	FBP	5.47/35.22	7.56/28.81	0.43/1.99	1.09/6.18
		SAFIRE 3	39.01/55.74	26.15/32.28	2.19/3.05	6.31/9.57
		SAFIRE 5	53.15/75.12	26.80/33.56	2.86/3.83	8.55/13.86
	2.65	FBP	4.77/28.46	7.66/34.53	0.42/2.05	1.14/5.51
		SAFIRE 3	29.84/43.10	72.11/83.53	1.81/2.42	5.17/7.24
		SAFIRE 5	41.70/60.21	99.74/117.36	2.18/3.01	6.54/9.12
	1.73	FBP	3.37/21.31	6.71/34.79	0.29/2.10	0.81/4.69
		SAFIRE 3	24.60/34.01	38.61/16.13	2.01/2.76	4.29/6.31
		SAFIRE 5	32.48/42.68	43.95/82.83	2.50/3.42	5.14/7.45
	1.00	FBP	2.88/14.80	5.93/34.36	0.28/1.38	0.71/3.61
		SAFIRE 3	16.35/16.90	35.87/48.83	1.27/1.89	3.29/4.75
		SAFIRE 5	21.95/23.53	46.67/72.57	1.60/2.41	3.79/5.72

ALU, aluminium; FBP, filtered back projection; HA, hydroxyapatite; SAFIRE, sinogram-affirmed iterative reconstruction; VEO, Trade name of a model-based iterative reconstruction.

include high-resolution image data with submillimetre accuracy in all three dimensions to enable precise multi-plane reconstructions, 3D volume rendering, 3D model printing and navigated surgery.[18] Sharp convolution kernels are applied to outline thin bone contours and trabecular structures, which is needed for the correct diagnosis and classification of fractures.[8] Orbital soft tissues including the optical nerve, or orbital muscles and fat are best evaluated using soft convolution kernels.[9] High contrast resolution and CNR are required for reliable diagnosis of posttraumatic entrapment of orbital fat or muscles.

In this study, phantom-based reference quality metrics from a clinically introduced ALADA dose protocol
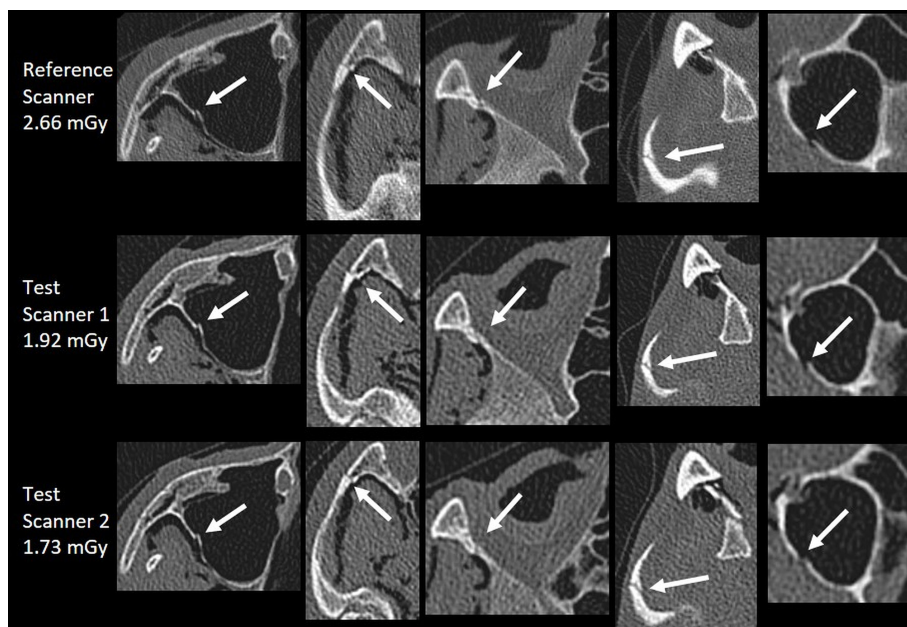
Figure 3 Comparative images of maxillofacial fractures of the cadaver study.

Table 3 AO-classification codes for cadaver heads 1 and 2. In cadaver 1, observer 1 misclassified a bony canal as fracture.

	AO-classification code	
	Observer 1	**Observer 2**
Cadaver head 1		
occipital	94O0m	94O0m
temporal right	/	/
frontal right + lateral midface right	92 Z1li.I1i.L1.Oli.m O(right) R(li).W1(li)2(i)	92 Z1li.I1i.L1.Oli.m O(right) R(li).W1(li) *a*
frontal left	92mOl.Z0l O(left) R(l). W1(l) 94m.F0 (R(s)	92 m.Ol.Z1l O(left) R(l). W1(l) *a*
temporal left	/	/
Cadaver head 2		
occipital	94O0m	94O0m
midface orbital inferior right	92 Z1l.I1.L1.Oli.U0 O(right) R(lim).W1(li)	92 Z1li.I1.L1.Oli.U0 O(right) R(lim).W1(li) *a*
central midface left	92 m.OI.L1.I1.Z1l O(left) R(l).W1(l)	92.m.Ol.L1.I1.Z1l O(left) R(l).W1(l)
mandibular head left	91 m.A1.P P(left) N1.B1	91 m.A1.P P(left) N1.B1

*a*difference in subclassification code, depicted in bold and italic.

for maxillofacial trauma at CTDI$_{vol}$ of 2.66 mGy were evaluated to help in the selection of potential ALADA dose protocols for other vendors and scanners. Identical settings of kV, mA, rotation time and pitch showed dose differences of 29–35% between the reference scanner and the two test scanners. These variances are explained by the many differences in scanner hardware, geometry, filter, acquisition parameters and reconstruction options, and underline the importance of reference image quality. Based on a simple descriptive comparison of the test and reference quality metrics, test protocols with the lowest dose showing non-inferiority of most of the metrics were suggested as ALADA dose protocols. For test scanner one, it was the protocol at 1.73 and for

scanner two the protocol at 1.92 mGy. Both protocols showed non-inferiority in the subsequent cadaver study.

Compared with the sharp bone kernel of the reference scanner, the selected bone kernels used in the test scanners could not provide similar spatial resolution and subjective sharpness scores, even at higher doses of 3.08–3.44 mGy. However, a spatial resolution of at least 2lp mm-1 seemed to be sufficient to enable the detection and classification of maxillofacial fractures similar to the reference protocol, as confirmed by the cadaver study. Based on the AO classifier system, only minor and non-clinically relevant differences in the classification or subclassification code were identified. The iterative reconstruction techniques SAFIRE 3, SAFIRE 5 and VEO did not improve the spatial resolution. In fact, iterative reconstruction techniques may produce texture changes and smoothing effects.[19–21] The third-generation adaptive statistical iterative reconstruction (ASIR) V may significantly improve smoothing effects and may provide equivalent or slightly superior spatial resolution than FBP.[22,23]

The contrast resolution scores of the soft kernel images of the test scanners were similar or better than the reference images. In test scanner 2, SAFIRE 3 and 5 could not improve scores. VEO outperformed FBP and SAFIRE and achieved the maximum scores in each group. Compared with the reference images, the HA-100 and HA-200 inserts showed lower CNR using FBP sharp kernel images. The results correlated with the subjective noise scores in scanner 1. The quality metrics of the phantom may thus be a valuable tool to quantify and benchmark contrast resolution and CNR for different doses, kernels and reconstruction techniques.

The phantom inserts best simulating CNR of ON and IRM were HA-100 and HA-200. In the cadavers, the FBP images of the test scanners showed CNR of both, ON and IRM similar to the FBP reference images. SAFIRE increased CNR but the results were not significantly better than the reference. VEO was superior over all other

Table 4 CNR of the optical nerve and inferior rectus muscle.

Scanner	*CTDIvol (mGy)*	*Reconstruction technology*	*Kernel*	*Optical nerve CNR (SD)*	*Inferior rectus muscle CNR (SD)*
Reference scanner	2.66	FBP	standard	2.80 (1.72)	2.36 (1.14)
		VEO	standard	10.18 (2.47) *b*	8.25 (2.91) *a*
			NR40	16.36 (3.03) *b*	10.60 (4.45) *b*
Test scanner 1	2.65	FBP	H30f	4.49 (0.75)	2.89 (0.60)
	1.92	FBP	H30f	3.98 (0.91)	4.19 (1.53)
Test scanner 2	2.65	FBP	H30f	4.17 (0.87)	4.67 (3.25)
		SAFIRE 3	J30f	5.12 (1.41)	5.47 (3.58)
		SAFIRE 5	J30f	5.90 (1.91)	6.01 (3.64)
	1.73	FBP	H30f	3.40 (0.81)	3.25 (1.33)
		SAFIRE 3	J30f	4.32 (1.08)	3.92 (1.69)
		SAFIRE 5	J30f	5.08 (1.41)	3.25 (2.03)

CNR, contrast-to-noise ratio; FBP, filtered back projection; LDP, low dose protocol; SAFIRE, Sinogram Affirmed Iterative Reconstruction; SD, standard deviation.
*a*Statistically significant (p < 0.05) difference to the reference scanner protocol FBP standard.
*b*Statistically significant (p < 0.001) difference to the reference scanner protocol FBP standard.
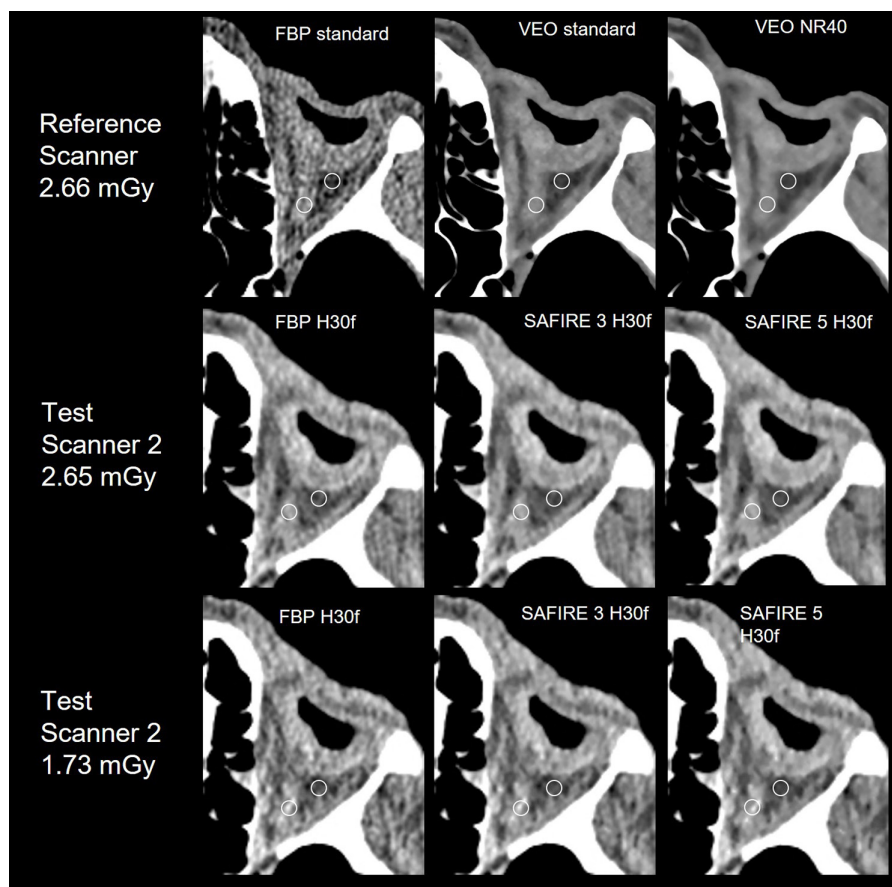
Figure 4 Comparative images of the left orbital soft tissues of the cadaver study. Circular region of interest used for CNR evaluation placed at the optical nerve (medial) and orbital fat (lateral). The inferior rectus muscle is not depicted on this slice.

reconstructions and provided significant higher CNR to the FBP reference. The results of iterative reconstructions were in line with published literature.[7,24–26]

The study has certain limitations. The used phantom does not simulate the complexity of human anatomy including trabecular and cortical bone, or different soft tissues. The cadaver heads were not fresh frozen and the conservation may affect radiological depiction of bone and soft tissues. Artifacts from head motion and dental fillings were not addressed. CT scanners allow for modification of numerous settings incl. kV, mAs, pitch, convolution kernels and selection of various iterative reconstructions. Therefore, for practical reasons, only a limited number of protocols could be tested in this study. Primary goal was to develop a simple approach to suggest ALADA dose protocols based on phantom testing in which image quality metrics should be non-inferior to the reference, rather than performing complex statistical testing, with probably limited clinical relevance. Evaluation of modulation transfer function and noise power spectrum could have improved the interpretation of sharpness and texture changes, respectively. The optimum set of phantom quality metrics and exact cut-off values that best predict clinical conditions still has to be defined.

Conclusion

Reference image quality metrics from phantom testing may be used for image quality benchmarking of potential ALADA dose protocols of different vendors and scanners. Such a reference quality approach may also be applied to other diagnostic CT examinations. The benefit for patients would be to receive CT examinations with the lowest diagnostically acceptable radiation doses, which are substantially lower than current DRLs.

REFERENCES

1. Tonkopi E, Duffy S, Abdolell M, Manos D. Diagnostic reference levels and monitoring practice can help reduce patient dose from CT examinations. *AJR Am J Roentgenol* 2017; **208**: 1073–81. https://doi.org/10.2214/AJR.16.16361
2. Raman SP, Johnson PT, Deshmukh S, Mahesh M, Grant KL, Fishman EK. CT dose reduction applications: available tools on the latest generation of CT scanners. *J Am Coll Radiol* 2013; **10**: 37–41. https://doi.org/10.1016/j.jacr.2012.06.025
3. Widmann G, Schullian P, Gassner EM, Hoermann R, Bale R, Puelacher W. Ultralow-dose CT of the craniofacial bone for navigated surgery using adaptive statistical iterative reconstruction and model-based iterative reconstruction: 2D and 3D image quality. *AJR Am J Roentgenol* 2015; **204**: 563–69. https://doi.org/10.2214/AJR.14.12766
4. Suomalainen A, Vehmas T, Kortesniemi M, Robinson S, Peltola J. Accuracy of linear measurements using dental cone beam and conventional multislice computed tomography. *Dentomaxillofac Radiol* 2008; **37**: 10–17. https://doi.org/10.1259/dmfr/14140281
5. Ludlow JB, Timothy R, Walker C, Hunter R, Benavides E, Samuelson DB, et al. Effective dose of dental CBCT-A meta analysis of published data and additional data for nine CBCT units. *Dentomaxillofac Radiol* 2015; **44**(1): 20140197. https://doi.org/10.1259/dmfr.20140197
6. Widmann G, Bischel A, Stratis A, Bosmans H, Jacobs R, Gassner E-M, et al. Spatial and contrast resolution of ultralow dose dentomaxillofacial CT imaging using iterative reconstruction technology. *Dentomaxillofac Radiol* 2017; **46**(4): 20160452. https://doi.org/10.1259/dmfr.20160452
7. Widmann G, Bischel A, Stratis A, Kakar A, Bosmans H, Jacobs R, et al. Ultralow dose dentomaxillofacial CT imaging and iterative reconstruction techniques: variability of hounsfield units and contrast-to-noise ratio. *Br J Radiol* 2016; **89**: 20151055. https://doi.org/10.1259/bjr.20151055
8. Widmann G, Dalla Torre D, Hoermann R, Schullian P, Gassner EM, Bale R, et al. Ultralow-dose computed tomography imaging for surgery of midfacial and orbital fractures using ASIR and MBIR. *Int J Oral Maxillofac Surg* 2015; **44**: 441–46. https://doi.org/10.1016/j.ijom.2015.01.011
9. Widmann G, Juranek D, Waldenberger F, Schullian P, Dennhardt A, Hoermann R, et al. Influence of ultra-low-dose and iterative reconstructions on the visualization of orbital soft tissues on maxillofacial CT. *AJNR Am J Neuroradiol* 2017; **38**: 1630–35. https://doi.org/10.3174/ajnr.A5239
10. Pauwels R, Stamatakis H, Manousaridis G, Walker A, Michielsen K, Bosmans H, et al. Development and applicability of a quality control phantom for dental cone-beam CT. *J Appl Clin Med Phys* 2011; **12**: 3478. https://doi.org/10.1120/jacmp.v12i4.3478
11. Riederer BM, Bolt S, Brenner E, Bueno-Lopez JL, Circulescu ARM, Davies DC, et al. The legal and ethical framework governing body donation in europe-1 st update on current practice. *Eur J Anat* 2012; **16**: 1–21.
12. Mchanwell S, Brenner E, Chirculescu ARM, Drukker J, Mameren H, Mazzotti G, et al. The legal and ethical framework governing body donation in europe-A review of current practice and recommendations for good practice. *Eur J Anat* 2008; **12**: 1–24.
13. Platzer W, Putz R, Poisel S. New system for the preservation and storage of anatomical matter. *Acta Anat (Basel)* 1978; **102**: 60–67. https://doi.org/10.1159/000145619
14. Audigé L, Cornelius CP, Kunz C, Buitrago-Téllez CH, Prein J. The comprehensive AOCMF classification system: classification and documentation within AOCOIAC software. *Craniomaxillofac Trauma Reconstr* 2014; **7**: S114–22. https://doi.org/10.1055/s-0034-1389564
15. Schegerer A, Loose R, Heuser LJ, Brix G. Diagnostic reference levels for diagnostic and interventional X-ray procedures in germany: update and handling. *Rofo* 2019; **191**: 739–51. https://doi.org/10.1055/a-0824-7603
16. UKHSA. UKHSA-RCE-1: doses from computed tomography (CT) exams in the UK - 2019 review. 2019.
17. Widmann G, Fasser M, Schullian P, Zangerl A, Puelacher W, Kral F, et al. Substantial dose reduction in modern multi-slice spiral computed tomography (MSCT) -guided craniofacial and skull base surgery. *Rofo* 2012; **184**: 136–42. https://doi.org/10.1055/s-0031-1281971
18. Widmann G. Image-Guided surgery and medical robotics in the cranial area. *Biomed Imaging Interv J* 2007; **3**(1): e11. https://doi.org/10.2349/biij.3.1.e11
19. Padole A, Ali Khawaja RD, Kalra MK, Singh S. Ct radiation dose and iterative reconstruction techniques. *AJR Am J Roentgenol* 2015; **204**: W384–92. https://doi.org/10.2214/AJR.14.13241
20. Al-Ekrish AA, Alfaleh W, Hörmann R, Alabdulwahid A, Puelacher W, Widmann G. Localization of the inferior alveolar canal using ultralow dose CT with iterative reconstruction techniques. *Dentomaxillofac Radiol* 2018; **47**(8): 20170477. https://doi.org/10.1259/dmfr.20170477
21. Al-Ekrish AA, Al-Shawaf R, Schullian P, Al-Sadhan R, Hörmann R, Widmann G. Validity of linear measurements of the jaws using ultralow-dose MDCT and the iterative techniques of ASIR and MBIR. *Int J Comput Assist Radiol Surg* 2016; **11**: 1791–1801. https://doi.org/10.1007/s11548-016-1419-y
22. Lim K, Kwon H, Cho J, Oh J, Yoon S, Kang M, et al. Initial phantom study comparing image quality in computed tomography using adaptive statistical iterative reconstruction and new adaptive statistical iterative reconstruction V. *J Comput Assist Tomogr* 2015; **39**: 443–48. https://doi.org/10.1097/RCT.0000000000000216
23. Euler A, Solomon J, Marin D, Nelson RC, Samei E. A third-generation adaptive statistical iterative reconstruction technique: phantom study of image noise, spatial resolution, lesion detectability, and dose reduction potential. *AJR Am J Roentgenol* 2018; **210**: 1301–8. https://doi.org/10.2214/AJR.17.19102
24. Schulz B, Beeres M, Bodelle B, Bauer R, Al-Butmeh F, Thalhammer A, et al. Performance of iterative image reconstruction in CT of the paranasal sinuses: a phantom study. *AJNR Am J Neuroradiol* 2013; **34**: 1072–76. https://doi.org/10.3174/ajnr.A3339
25. Widmann G, Al-Shawaf R, Schullian P, Al-Sadhan R, Hörmann R, Al-Ekrish AA. Effect of ultra-low doses, ASIR and MBIR on density and noise levels of MDCT images of dental implant sites. *Eur Radiol* 2017; **27**: 2225–34. https://doi.org/10.1007/s00330-016-4588-8
26. Hoxworth JM, Lal D, Fletcher GP, Patel AC, He M, Paden RG, et al. Radiation dose reduction in paranasal sinus CT using model-based iterative reconstruction. *AJNR Am J Neuroradiol* 2014; **35**: 644–49. https://doi.org/10.3174/ajnr.A3749